

RAPID REPORT

POTENTIATION OF THE NICOTINIC ACETYLCHOLINE RECEPTOR BY ALUMINUM IN MAMMALIAN NEURONS

W.-P. HU,^{a*} X.-M. LI,^a J.-G. CHEN^c AND Z.-W. LI^{b**}

^aDepartment of Physiology, Xianning College, Xianning 437100, PR China

^bDepartment of Neurobiology, Tongji Medical College of Huazhong University of Science and Technology, Wuhan 430030, PR China

^cDepartment of Pharmacology, Tongji Medical College of Huazhong University of Science and Technology, Wuhan 430030, PR China

Abstract—Aluminum (Al³⁺), a known neurotoxic substance, has long been implicated in the pathogenesis of Alzheimer's disease and other neurodegenerative diseases. Al³⁺ targets many ligand-gated and voltage-gated ion channels and modulates their functions. In the present study, the actions of Al³⁺ on the nicotinic acetylcholine receptor (nAChR) were investigated by whole-cell patch clamp technique in acutely isolated rat trigeminal ganglion neurons. We observed that Al³⁺ potentiated nicotine-evoked inward currents in a concentration-dependent manner (10–1000 μ M). The effects of Al³⁺ on nicotine-evoked currents were voltage independent. Al³⁺ appeared to increase the affinity of nicotine to nAChR but not the efficacy. Al³⁺ reduced the agonist concentration producing a half-maximal response (EC₅₀) for nicotine from 74.4 \pm 1.9 μ M to 32.9 \pm 2.6 μ M, but did not alter the threshold nor maximal response. On the contrary, another trivalent cation, Ga³⁺, had little effect on nicotine-evoked currents. The present results indicated that Al³⁺ enhanced the function of nAChR and this potentiation might underlie the neurological alteration induced by Al³⁺. © 2007 IBRO. Published by Elsevier Ltd. All rights reserved.

Key words: aluminum, nicotinic acetylcholine receptor, potentiation, current, neuron.

Aluminum (Al³⁺) is the most abundant and widely distributed metal in the earth's crust. It enters the human body via food, air, water and drugs such as antacids or deodorants,

etc. Our daily intake of Al³⁺ is estimated to be approximately 10–20 mg (Edwardson et al., 1992). Al³⁺ could permeate the blood–brain barrier and accumulate in the brain (Yokel, 2002). The concentration of Al³⁺ was 0.5–3 mM in the brain of a dementia patient (Good et al., 1992). Elevated levels of the brain Al³⁺ have been reported in Alzheimer's disease, amyotrophic lateral sclerosis, Guam-Parkinson's dementia, etc. (Crapper et al., 1973; Perl et al., 1982; Kawahara, 2005). Al³⁺ is neurotoxic and is considered today as a putative etiological factor in these neurodegenerative diseases (Miu and Benga, 2006).

Nicotinic acetylcholine receptors (nAChRs) belong to the superfamily of ligand-gated ion channels and are widely distributed throughout the CNS and peripheral nervous system (Keiger and Walker, 2000). Neuronal nAChRs participate in a diverse array of physiological processes including attention, learning and memory (Ji et al., 2001; Ge and Dani, 2005). Alteration of neuronal nAChR function has been implicated in various neuronal disorders, such as schizophrenia, epilepsy, Alzheimer's disease, dementia with Lewy bodies, Down syndrome, and Parkinson's disease (Dani and Bertrand, 2007). Many substances modulate nAChR function by binding to allosteric sites distinct from the ACh-binding site. For instance, nAChRs possess binding sites for multivalent cations. In previous studies it has been shown that di- and trivalent cations exert modulation on nAChRs; for instance, currents mediated by nAChRs are potentiated by Zn²⁺, Ca²⁺ or Ba²⁺, and inhibited by Pb²⁺ or La³⁺ (Garcia-Colunga and Miledi, 1997; Oortgiesen et al., 1997; Hsiao et al., 2006; McLaughlin et al., 2006). Sensory neurons, including trigeminal ganglion (TG) neurons, express a variety of nAChR subtypes (Liu et al., 1993; Flores et al., 1996). In the present study, we found that Al³⁺ potentiated nicotine-activated currents (I_{nic}), using peripheral TG neuron as an accessible model.

EXPERIMENTAL PROCEDURES

Isolation of TG neurons

The experimental protocol was approved by the animal research ethics committee of Xianning College. All procedures conformed to international guidelines on the ethical use of animals, and every effort was made to minimize the number of animals used and their suffering. Isolating methods have been described in detail previously (Hu et al., 2004, 2005). In brief, 2- to 3-week-old Sprague-Dawley rats were anesthetized with ether and then decapitated. The TGs were taken out and transferred immediately into Dulbecco's Modified Eagle Medium (DMEM, Sigma, St. Louis, MO, USA) at pH 7.4. After the removal of the surrounding connective tissues,

*Corresponding author. Tel: +86-715-8261016.

E-mail address: wangping_hu@yahoo.com (W.-P. Hu).

**Correspondence to: Z.-W. Li, Department of Neurobiology, Tongji Medical College, Huazhong University of Science and Technology, 13 Hangkong Road, Wuhan 430030, PR China. Tel: +86-27-83692340; fax: +86-27-83693761.

E-mail address: zhiwangli@yahoo.com (Z.-W. Li).

Abbreviations: Al³⁺, aluminum; Atr, atropine; DMEM, Dulbecco's Modified Eagle medium; DMPP, dimethylphenylpiperazinium; EC₅₀, agonist concentration producing a half-maximal response; EGTA, ethylene glycol-bis(2-aminoethyl ether)-N,N,N',N'-tetraacetic acid; Ga³⁺, gallium; GDP- β -S, guanosine 5'-O-(2-thiodiphosphate); Hepes, N-(2-hydroxyethyl)piperazine-N'-(2-ethanesulfonic acid); Hex, hexamethonium; I_{nic}, nicotine-activated current; I_{nic(p)}, peak values of nicotine-activated current; I_{nic(ss)}, steady state component of nicotine-activated current; I-V, current-voltage; nAChR, nicotinic acetylcholine receptor; TG, trigeminal ganglion; Tub, tubocurarine; α -BTx, α -bungarotoxin.

the TGs were minced with fine spring scissors and the ganglion fragments were placed in a flask containing 5 ml of DMEM with trypsin (type II-S, Sigma, 0.5 mg/ml), collagenase (type I-A, Sigma, 1.0 mg/ml), DNase (type IV, Sigma, 0.1 mg/ml), and incubated at 35 °C in a shaking waterbath for 30–35 min. Soybean trypsin inhibitor (type II-S, Sigma, 1.25 mg/ml) was then added to stop trypsin digestion. Dissociated neurons were placed in a 35-mm Petri dish and kept for at least another 30 min before electrophysiological recording. The neurons selected for patch clamp experiment were 15–45 μm in diameter.

Electrophysiological recordings

Whole-cell patch clamp recordings were carried out at room temperature (22–24 °C) using a whole cell/patch clamp amplifier (CEZ-2400, Nihon, Koden, Tokyo, Japan). The pipettes were filled with internal solution containing (mM): KCl 140, CaCl_2 1, MgCl_2 2.5, Hepes 10, EGTA 11 and ATP 5; its pH was adjusted to 7.2 with KOH and osmolarity was adjusted to 310 mOsm/L with sucrose. Cells were bathed in an external solution containing (mM): NaCl 150, KCl 5, CaCl_2 2.5, MgCl_2 2, Hepes 10, D-glucose 10; its osmolarity was adjusted to 340 mOsm/L with sucrose and pH was adjusted to 7.4 with NaOH. The resistance of the recording pipette was in the range of 2–5 M Ω . A small patch of membrane underneath the tip of the pipette was aspirated to form a gigaseal and then a more negative pressure was applied to rupture it, thus establishing a whole-cell configuration. The adjustment of capacitance compensation and series resistance compensation was done before recording the membrane currents. The holding potential was set at –60 mV, except when indicated specially. Membrane currents were filtered at 10 kHz (–3dB), and the data were recorded by a pen recorder (Nihon Kohden).

Drug application

Drugs used in the experiments were purchased from Sigma Chemical Co. and include: Al^{3+} trichloride, gallium (Ga^{3+}) trichloride, (\pm)-nicotine, dimethylphenylpiperazinium (DMPP), hexamethonium (Hex), (+) tubocurarine (Tub), α -bungarotoxin (α -BTx), atropine (Atr). All drugs were dissolved in the external solution just before use and held in a linear array of fused silica tubes (o.d./i.d.=500 μm /200 μm) connected to a series of independent reservoirs. The distance from the tube mouth to the cell examined was around 100 μm . The application of each drug could be driven by gravity and controlled by the corresponding valve, and rapid solution exchange could be achieved within about 150 ms by shifting the tubes horizontally with a micromanipulator. Cells were constantly bathed in normal external solution flowing from one tube connected to a larger reservoir between drug applications. In some experiments, guanosine 5'-O-(2-thiodiphosphate) (GDP- β -S, Sigma) that needed to be applied intracellularly was dissolved in the internal solution.

Statistical analysis

Data were statistically compared using the Student's *t*-test or analysis of variance followed by the Bonferroni's post hoc test. Statistical analysis of concentration–response data was performed using non-linear curve-fitting program ALLFIT. Current values are expressed as means \pm S.E.M.

RESULTS

Neurons isolated freshly from rat TGs were round or elliptical in shape and their diameters were in the range of 15–45 μm . Most of the neurons examined (82.1%, 55/67) responded to externally applied nicotine with a concentration-dependent (10–1000 μM) inward current. The 100 μM I_{nic} can be mimicked by agonist DMPP (100 μM , $n=7$), and

blocked by antagonist (+)-Tub (100 μM , $n=9$) and nicotinic receptor blocker, Hex (100 μM , $n=9$) markedly (Fig. 1A). In contrast, α -BTx (1 μM , $n=13$), a toxin that binds in a pseudo-irreversible fashion to neuronal nicotinic receptors, and Atr (100 μM , $n=9$), a cholinergic receptor antagonist, had no effect on I_{nic} (Fig. 1A).

No detectable change in membrane current was observed when Al^{3+} was applied alone in the present study ($n=10$). However, in the presence of Al^{3+} , the peak values of nicotine-activated current ($I_{\text{nic}(p)}$) rose stepwise with the increase of Al^{3+} from 10 to 1000 μM and reached the maximum at 1000 μM (Fig. 1B, C). It is noteworthy that the increase in $I_{\text{nic}(p)}$ was more evident than the increase in steady state component of nicotine-activated current ($I_{\text{nic}(ss)}$), in fact, the amplitude of the latter even decreased (Fig. 1B, C). In other words, the desensitization of I_{nic} was enhanced with the increase of co-applied Al^{3+} . To address whether the results were specific for Al^{3+} , we tested another tri-valent cation, Ga^{3+} , on I_{nic} . In the presence of Ga^{3+} (30, 100 or 1000 μM , $n=6–8$) both the peak values and the steady state components of 100 μM I_{nic} changed slightly (within 3.2%–4.8% of the control), suggesting no effect of Ga^{3+} on I_{nic} .

Fig. 2A showed that the magnitude of Al^{3+} enhancement was dependent upon the nicotine concentration. Fig. 2B illustrated that Al^{3+} shifted the nicotine concentration–response curve to the left, reducing the agonist concentration producing a half-maximal response (EC_{50}) for nicotine from 74.4 ± 1.9 μM in the absence of Al^{3+} to 32.9 ± 2.6 μM in the presence of 100 μM Al^{3+} ($n=12$, $P<0.01$, unpaired *t*-test). Al^{3+} did not alter the slope or Hill coefficient ($n=1.75$ in the absence of Al^{3+} vs. $n=1.81$ in the presence of Al^{3+}), the threshold or maximal value of the nicotine concentration–response curve ($n=12$, $P>0.1$, Bonferroni's post hoc test). Fig. 2C showed that in the double reciprocal plot of the potentiation of I_{nic} by Al^{3+} , it was evident that Al^{3+} potentiated I_{nic} by changing the apparent affinity of the nAChRs for nicotine.

Moreover, when 500 μM GDP- β -S, a non-hydrolysable GDP analog, was included in the recording pipette for intracellular dialysis, the potentiation of 100 μM I_{nic} by 100 μM Al^{3+} ($45.4 \pm 6.6\%$, $n=9$) was comparable to that of control ($49.1 \pm 6.8\%$; $n=9$, $P>0.1$, paired *t*-test), thus ruling out the involvement of G-protein signal pathways in the potentiation of I_{nic} by Al^{3+} .

To investigate whether the actions of Al^{3+} on nAChR are dependent on membrane potential, we studied the potentiation of I_{nic} by Al^{3+} at various holding potential conditions. The current–voltage (*I*–*V*) relationships for 100 μM I_{nic} in the absence and presence of 100 μM Al^{3+} are demonstrated in Fig. 3B. Both curves manifested the characteristic of strong inward rectification and there were no clear reversals, due mainly to the rectifying characteristics of the channel itself. Al^{3+} enhanced I_{nic} at all holding potentials between –80 and 0 mV as shown by the increase of the slope of the *I*–*V* curve (Fig. 3A, B). Fig. 3C showed the effect of membrane potential on Al^{3+} enhancement of I_{nic} . The effect of Al^{3+} on membrane conductance did not differ significantly at membrane holding potentials between –80 and 0 mV ($n=8$, $P>0.1$, analysis of variance).

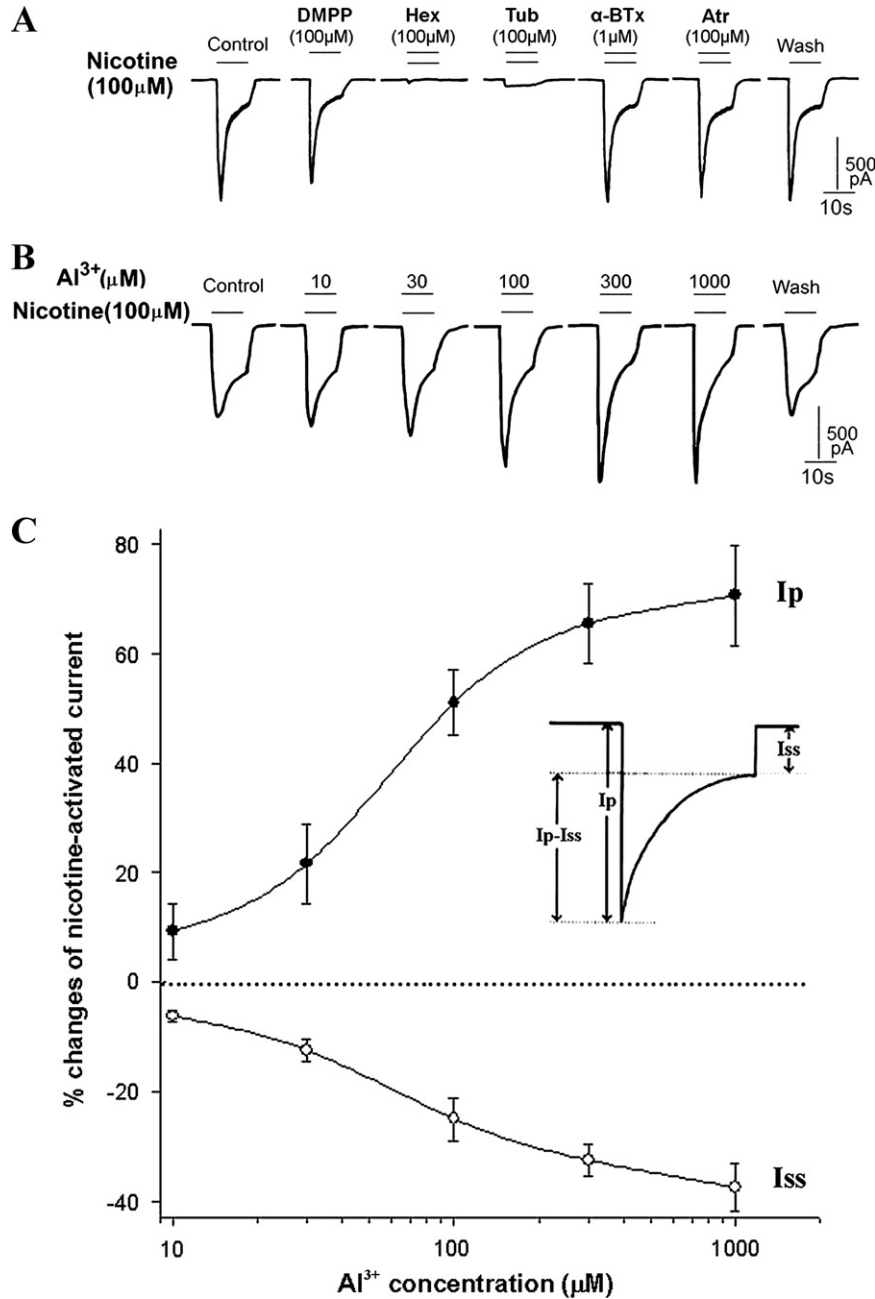


Fig. 1. Concentration-dependent potentiation of I_{nic} by Al^{3+} . (A) Inward current evoked by 100 μM nicotine (I_{nic}) could be mimicked by nAChR agonist DMPP, and blocked by nAChR antagonist (+)-Tub and nAChR blocker Hex, while α -BTx, a neurotoxin which binds irreversibly to AChR, and Atr, an antagonist of cholinergic receptor, had no effect on I_{nic} . All current traces were recorded from the same TG neuron. In each experiment, I_{nic} recovered to its control amplitude after washout ($n=7-13$). (B) Sequential current traces (from left to right) illustrate the potentiation of 100 μM I_{nic} by different concentrations of Al^{3+} (10–1000 μM) on a single TG neuron. (C) Concentration-dependence modulation of 100 μM I_{nic} by Al^{3+} (10–1000 μM). The $I_{nic(p)}$ increased with the increase of Al^{3+} concentration, while the $I_{nic(ss)}$ decreased. Each point represents the mean \pm S.E.M. of 8 to 12 TG neurons with membrane potential clamped at -60 mV. The inset schematic diagram shows the individual components of I_{nic} , i.e. I_p and I_{ss} .

These results indicated that Al^{3+} potentiated the activity of neuronal nAChRs in a voltage-independent manner.

DISCUSSION

We found that I_{nic} are potentiated by Al^{3+} in a concentration-dependent manner in the present study. Firstly, the I_{nic} recorded in TG neurons were mediated by α -BTx-insensitive

nAChR, since it could be mimicked by nAChR agonist DMPP and blocked by nAChR antagonists (+)-Tub and Hex, but not by α -BTx and Atr. The characteristics of nAChR-mediated current recorded in this work were identical to the currents recorded by Liu et al. (1993) in rat TG neurons. Secondly, the potentiation of nAChRs was specific for Al^{3+} , since another trivalent cation Ga^{3+} has little effect on nAChRs.

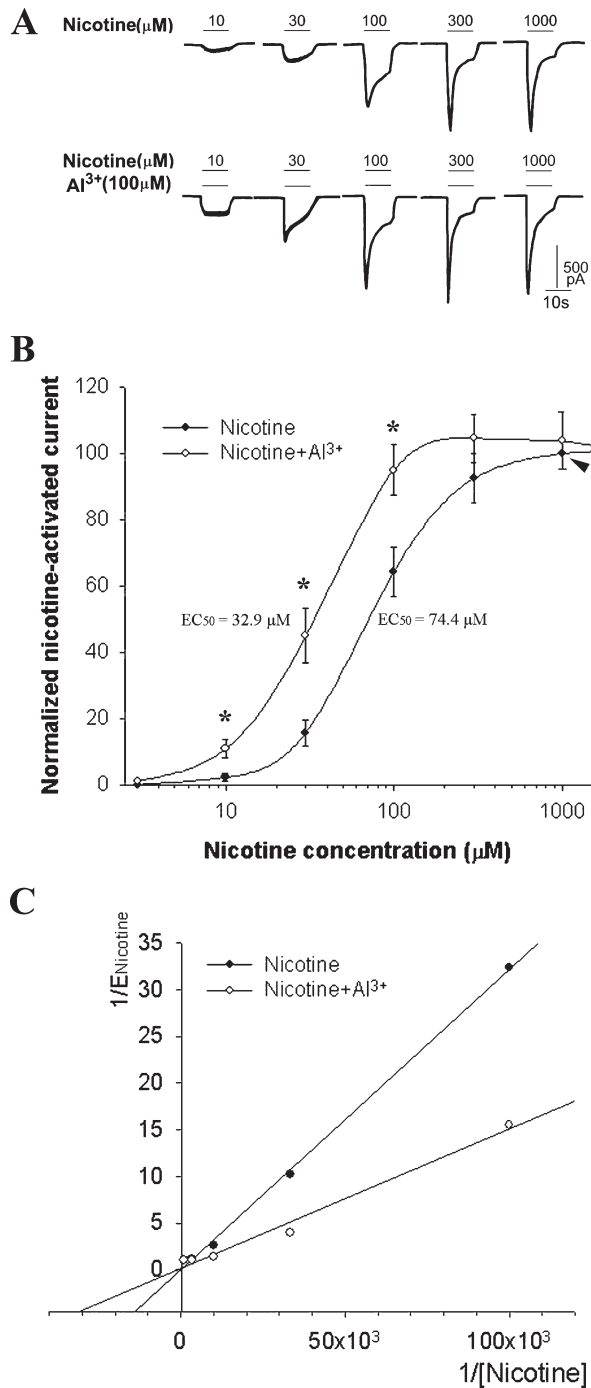


Fig. 2. Concentration–response relationships for nicotine with and without Al³⁺ co-application. (A) I_{nic} evoked by nicotine (10–1000 μM) in the absence of Al³⁺ (upper row) and presence of 100 μM Al³⁺ (lower row). (B) Concentration–response curves for nicotine without and with Al³⁺ co-application. Al³⁺ shifts the concentration–response curve for nicotine leftwards obviously. All current values were normalized to the current response induced by 1000 μM nicotine alone at the holding potential of -60 mV (marked with arrowhead). Each point represents the mean \pm S.E.M. of I_{nic} of 8 to 12 neurons. * $P < 0.05$, analysis of variance followed by Bonferroni's post hoc test. (C) The double reciprocal plot. All data were obtained from the graph (B).

The present study showed that 100 μM Al³⁺ shifted the nicotine concentration–response curve leftwards evidently, with a significant decrease in the EC₅₀ and no change in minimal and maximal values of the curve. These observations suggested that Al³⁺ increased the apparent affinity of nAChR, similar to our previous observation on potentiation I_{ATP} by Zn²⁺ (Li et al., 1993). A possibility is that Al³⁺ increases the probability of receptor channel opening, like the actions of La³⁺ on muscle AChRs and Zn²⁺ on nAChRs (Garcia-Colunga and Miledi, 1997; Hsiao et al., 2006). The enhancing effect of 100 μM Al³⁺ was not affected by GDP- β -S, a non-hydrolysable GDP analog, indicating no involvement of G protein–dependent signal pathways. We think the Al³⁺ modulation may be direct allosteric modulation of the receptor protein rather than second-messenger mediated. It has been shown that neuronal nAChRs possess Zn²⁺ and Ca²⁺ binding sites and their function is enhanced by these cations (Hsiao et al., 2006; McLaughlin et al., 2006). It was unlikely that the Al³⁺ action on nAChRs was mediated by a surface charge screening effect, since the effect of Al³⁺ was not mimicked by the same concentration of Ga³⁺, and the potentiation of nAChRs by Al³⁺ was independent of membrane potential. Thus, the external surface of nAChR channels in mammalian neurons may possess a site through which Al³⁺ augments the response to nicotine. In the present study, Al³⁺ not only enhanced the peak currents evoked by 100 μM nicotine but also decreased the amplitudes of steady state current, suggesting that Al³⁺ may accelerate the desensitization of nicotine-evoked current. It is reported that $\alpha 3\beta 4$ is the dominant nAChR subtype in TG neurons (Flores et al., 1996). Abdrakhmanova et al. (2002) reported that protons have similar desensitizing effects on the recombinant rat $\alpha 3\beta 4$ nAChR, and the accelerated desensitization results in the enhancement of the reactivated nicotinic current. The exact mechanism underlying the effects of Al³⁺ on nAChRs remains to be explored.

Reportedly, Al³⁺ can exert different modulation on other ligand-gated and voltage-gated ion channels, although some of the results are still controversial. It has been reported that Al³⁺ is a potent blocker of voltage-activated calcium channel current with an IC₅₀ near 85 μM in rat dorsal root ganglion neurons (Busselberg et al., 1993; Platt and Busselberg, 1994). These effects of Al³⁺ on calcium channel currents appear to be pH-dependent, i.e. low pH increases the sensitivity of the channel to Al³⁺. Al³⁺ also inhibits voltage-activated sodium and potassium currents in the hippocampal neurons (Zhang et al., 2004). In contrast, Busselberg et al. (1993) have suggested that Al³⁺ has little effect on sodium or potassium channels, although it blocks calcium channel currents. Kanazirska et al. (1997) have reported that 100 μM Al³⁺ inhibits sodium channels from rat hippocampal neurons, although it has little effect on potassium channels. In addition, Al³⁺ blocks the currents mediated by all glutamate ionotropic receptors (NMDA and AMPA/kainate receptors) (Platt et al., 1994). Furthermore, Al³⁺ impairs long-term potentiation, the processes involved in memory, in the hippocampus (Platt et al., 1995). It has been reported that Al³⁺ enhances gluta-

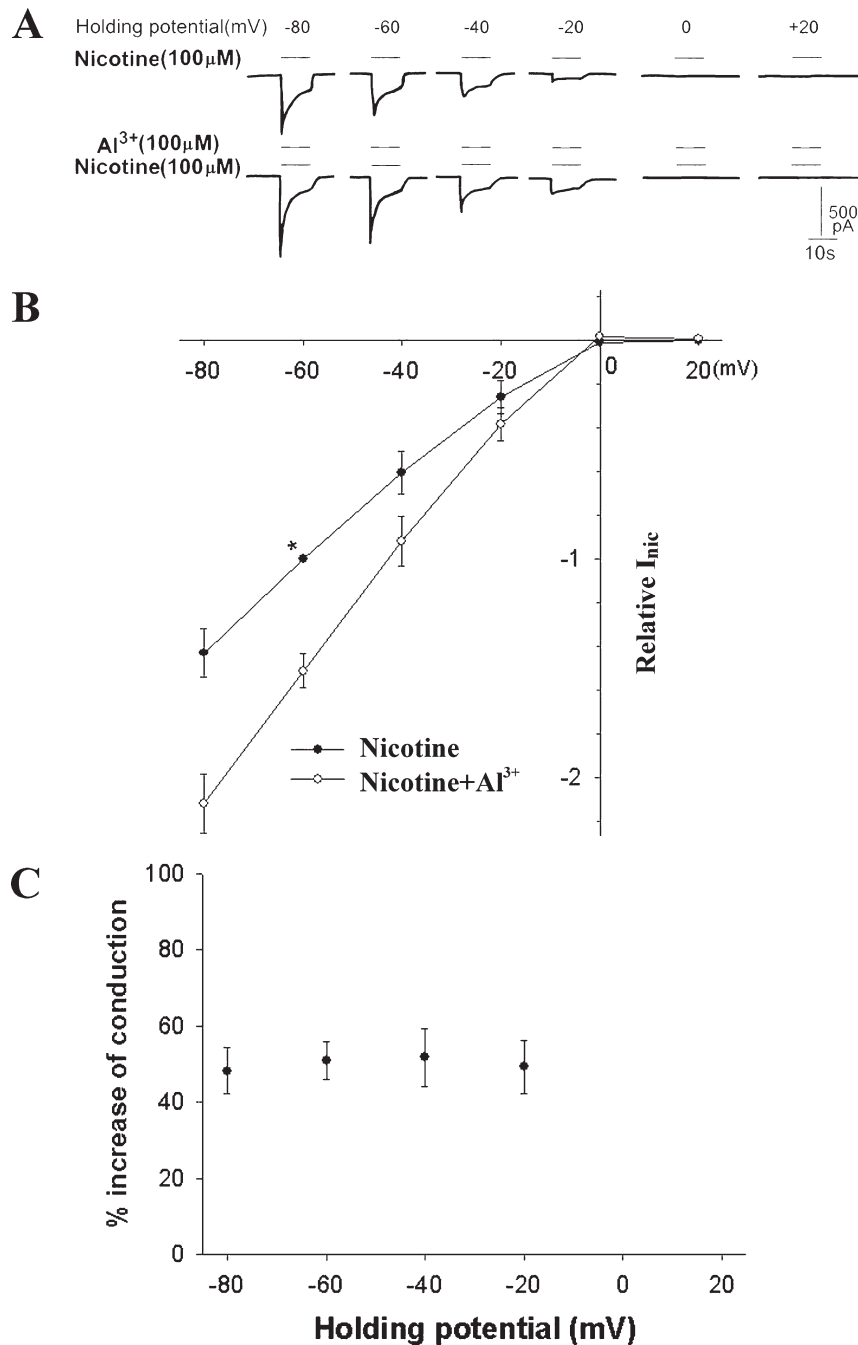


Fig. 3. I–V relationships for I_{nic} with and without Al^{3+} co-application. (A) I_{nic} with co-application of Al^{3+} (lower row) compared with the control (upper row) at different holding potentials ranging from -80 to $+20$ mV. (B) I–V curves for I_{nic} with or without Al^{3+} co-application. All current values were normalized to the current response induced by $100 \mu M$ nicotine at the holding potential of -60 mV (marked with asterisk). Each point represents the mean \pm S.E.M. (C) Increase of conductance (%) evoked by Al^{3+} was independent of holding potentials.

mate-mediated excitotoxicity in culture hippocampal neurons (Matyja, 2000). Trombley (1998) has reported that Al^{3+} has little effect on currents evoked by the amino acid receptor agonists glutamate, kainate and NMDA, however, Al^{3+} selectively modulates $GABA_A$ receptor-mediated current in the mammalian olfactory system. High concentration Al^{3+} blocks $GABA$ -evoked currents, however, low concentration Al^{3+} potentiates $GABA$ -evoked currents.

The accumulation of Al^{3+} in the brain and the decline of nAChRs functions contribute to Alzheimer's and other forms of dementia (Kawahara, 2005; Dani and Bertrand, 2007), so we presumed that Al^{3+} would inhibit the function of nAChR. It was surprising that nicotine-evoked currents were potentiated by Al^{3+} in the TG neurons in the present study. To date, nine α and three β subunits of nAChRs have been identified. $\alpha 3\beta 4$ is the dominant subtype of

nAChR in the TG neurons, whereas the most abundant forms of nAChRs in the CNS are $\alpha 4\beta 2$ and $\alpha 7$ (Flores et al., 1996; Smythies, 2005). We inferred that Al^{3+} might have different effects on distinct nAChR subtypes. Our present results may not generalize to the nAChRs in the CNS. Thus, further investigations employing neurons isolated from the brain would be necessary to fully understand the probable connection of Al^{3+} and nAChRs in the development of dementia.

REFERENCES

- Abdrakhmanova G, Dorfman J, Xiao Y, Morad M (2002) Protons enhance the gating kinetics of the $\alpha 3\beta 4$ neuronal nicotinic acetylcholine receptor by increasing its apparent affinity to agonists. *Mol Pharmacol* 61:369–378.
- Busselberg D, Platt B, Haas HL, Carpenter DO (1993) Voltage gated calcium channel currents of rat dorsal root ganglion (DRG) cells are blocked by Al^{3+} . *Brain Res* 622:163–168.
- Crapper DR, Krishnan SS, Dalton AJ (1973) Brain aluminum distribution in Alzheimer's disease and experimental neurofibrillary degeneration. *Science* 180:511–513.
- Dani JA, Bertrand D (2007) Nicotinic acetylcholine receptors and nicotinic cholinergic mechanisms of the central nervous system. *Annu Rev Pharmacol Toxicol* 47:699–729.
- Edwardson JA, Candy JM, Ince PG, McArthur FK, Morris CM, Oakley AE, Taylor GA, Bjertness E (1992) Aluminium accumulation, beta-amyloid deposition and neurofibrillary changes in the central nervous system. *Ciba Found Symp* 169:165–179; discussion 179–185.
- Flores CM, DeCamp RM, Kilo S, Rogers SW, Hargreaves KM (1996) Neuronal nicotinic receptor expression in sensory neurons of the rat trigeminal ganglion: demonstration of $\alpha 3\beta 4$, a novel subtype in the mammalian nervous system. *J Neurosci* 16:7892–7901.
- Garcia-Colunga J, Miledi R (1997) Opposite effects of lanthanum on different types of nicotinic acetylcholine receptors. *Neuroreport* 8:3293–3296.
- Ge S, Dani JA (2005) Nicotinic acetylcholine receptors at glutamate synapses facilitate long-term depression or potentiation. *J Neurosci* 25:6084–6091.
- Good PF, Perl DP, Bierer LM, Schmeidler J (1992) Selective accumulation of aluminum and iron in the neurofibrillary tangles of Alzheimer's disease: a laser microprobe (LAMMA) study. *Ann Neurol* 31:286–292.
- Hsiao B, Mihalak KB, Repicky SE, Everhart D, Mederos AH, Malhotra A, Luetje CW (2006) Determinants of zinc potentiation on the $\alpha 4$ subunit of neuronal nicotinic receptors. *Mol Pharmacol* 69:27–36.
- Hu WP, Guan BC, Ru LQ, Chen JG, Li ZW (2004) Potentiation of 5-HT₃ receptor function by the activation of coexistent 5-HT₂ receptors in trigeminal ganglion neurons of rats. *Neuropharmacology* 47:833–840.
- Hu WP, Li XM, Wu JL, Zheng M, Li ZW (2005) Bradykinin potentiates 5-HT₃ receptor-mediated current in rat trigeminal ganglion neurons. *Acta Pharmacol Sin* 26:428–434.
- Ji D, Lape R, Dani JA (2001) Timing and location of nicotinic activity enhances or depresses hippocampal synaptic plasticity. *Neuron* 31:131–141.
- Kanazirska M, Vassilev PP, Birzon SY, Vassilev PM (1997) Voltage-dependent effect of Al^{3+} on channel activities in hippocampal neurons. *Biochem Biophys Res Commun* 232:84–87.
- Kawahara M (2005) Effects of aluminum on the nervous system and its possible link with neurodegenerative diseases. *J Alzheimers Dis* 8:171–182, discussion 209–115.
- Keiger CJ, Walker JC (2000) Individual variation in the expression profiles of nicotinic receptors in the olfactory bulb and trigeminal ganglion and identification of $\alpha 2$, $\alpha 6$, $\alpha 9$, and $\beta 3$ transcripts. *Biochem Pharmacol* 59:233–240.
- Li C, Peoples RW, Li Z, Weight FF (1993) Zn^{2+} potentiates excitatory action of ATP on mammalian neurons. *Proc Natl Acad Sci U S A* 90:8264–8267.
- Liu L, Pugh W, Ma H, Simon SA (1993) Identification of acetylcholine receptors in adult rat trigeminal ganglion neurons. *Brain Res* 617:37–42.
- Matyja E (2000) Aluminum enhances glutamate-mediated neurotoxicity in organotypic cultures of rat hippocampus. *Folia Neuropathol* 38:47–53.
- McLaughlin JT, Fu J, Sproul AD, Rosenberg RL (2006) Role of the outer beta-sheet in divalent cation modulation of $\alpha 7$ nicotinic receptors. *Mol Pharmacol* 70:16–22.
- Miu AC, Benga O (2006) Aluminum and Alzheimer's disease: a new look. *J Alzheimers Dis* 10:179–201.
- Oortgiesen M, van Kleef RG, Vijverberg HP (1997) Dual, non-competitive interaction of lead with neuronal nicotinic acetylcholine receptors in N1E-115 neuroblastoma cells. *Brain Res* 747:1–8.
- Perl DP, Gajdusek DC, Garruto RM, Yanagihara RT, Gibbs CJ (1982) Intraneuronal aluminum accumulation in amyotrophic lateral sclerosis and Parkinsonism-dementia of Guam. *Science* 217:1053–1055.
- Platt B, Busselberg D (1994) Actions of aluminum on voltage-activated calcium channel currents. *Cell Mol Neurobiol* 14:819–829.
- Platt B, Carpenter DO, Busselberg D, Reymann KG, Riedel G (1995) Aluminum impairs hippocampal long-term potentiation in rats in vitro and in vivo. *Exp Neurol* 134:73–86.
- Platt B, Haas H, Busselberg D (1994) Aluminium reduces glutamate-activated currents of rat hippocampal neurones. *Neuroreport* 5:2329–2332.
- Smythies J (2005) Section I. The cholinergic system. *Int Rev Neurobiol* 64:1–122.
- Trombley PQ (1998) Selective modulation of GABA_A receptors by aluminum. *J Neurophysiol* 80:755–761.
- Yokel RA (2002) Brain uptake, retention, and efflux of aluminum and manganese. *Environ Health Perspect* 110 (Suppl 5):699–704.
- Zhang B, Nie A, Bai W, Meng Z (2004) Effects of aluminum chloride on sodium current, transient outward potassium current and delayed rectifier potassium current in acutely isolated rat hippocampal CA1 neurons. *Food Chem Toxicol* 42:1453–1462.